

Reconstruction of Real Size Distributions Hidden in Phase-Doppler Anemometry Results Obtained from Droplets of Inhomogeneous Liquids

Uwe Manasse*, Thomas Wriedt**, Klaus Bauckhage**

(Received: 27 September 1993)

Abstract

Real process fluids such as emulsions and suspensions are optically absorbent as well as inhomogeneous. Using phase-Doppler anemometry (PDA) for investigating the spray cone, the inhomogeneities have led to incomprehensible size distributions. In this paper, solutions of instant coffee and condensed milk, representing typical process fluids, were chosen for PDA measurements in comparison with PDA applied to water droplets with the same atomization process in order to clarify the

reasons for the measured broad size distributions. By applying PDA to monodisperse droplets and to "monodisperse" and real polydisperse sprays consisting of such fluids, it is shown how the measured size distributions arise. Based on this knowledge, the real size distributions are reconstructed and compared with that of water atomization. Therefore, PDA can in future also be applied to real process fluids, and process control, based on the information provided by PDA, is coming nearer.

1 Introduction

Phase-Doppler anemometry (PDA) is a well established optical tool for non-intrusive, simultaneous measurements of the velocity and size of spherical particles generated, for instance, by spraying optically homogeneous materials. These materials can be either transparent or opaque. Examples of such media are water, oil and strongly reflecting liquids such as molten metals. However, difficulties arise in applying PDA to real process fluids such as emulsions and suspensions which are often optically absorbent and inhomogeneous. Examples are highly concentrated liquids processed by spray drying. Optical inhomogeneity of the sprayed fluid will result in a broadening of the particle size distributions measured by PDA. In the past, it has been demonstrated that detecting the reflected instead of the refracted light reduces the disturbing influence of the inhomogeneities [1]. However, owing to the low scattered light intensities, the very small droplets are often not detectable. High scattered light intensities exist only in the forward direction, i.e. where the refracted light dominates.

Using an infrared laser in a PDA set-up, the disturbances, resulting from the inhomogeneities inside the droplets, in the detected refracted light are reduced, because the ratio between laser wavelength and diameter of the inhomogeneities increases [2]. Although the influence of the inhomogeneities (finely dispersed fat globules, solid particles or impurities) within a droplet to be sized is decreased, the measured size distributions

are hardly interpretable. However, if the formation process of the measured size distributions can be clarified, it should be possible to discover information about the real size distributions.

2 Nozzle Results

Figures 1 and 2 show size distributions as a result of PDA measurements conducted 30cm below a flat cone nozzle in the centre of the spray cone. Distilled water, and 8% solutions of condensed milk and of instant coffee were sprayed at a liquid pressure of 3 bar. The PDA measurements were carried out at an off-axis angle of 30° (detection of refracted light) using laser wavelengths of 488 and 830nm. Since the solutions were of low concentration their properties such as viscosity, surface tension and density should be similar to those of water. Therefore, the "real" size distributions of the sprayed process fluids should not be much different from the water size distribution. Even if the influence of

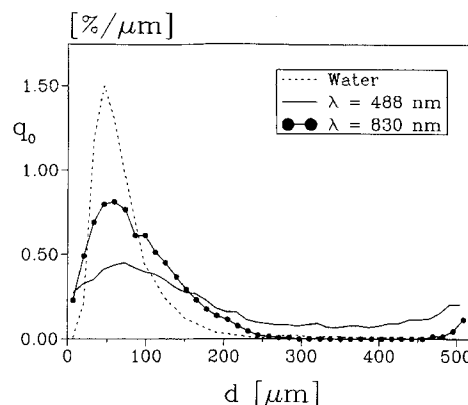


Fig. 1: Size distributions achieved by PDA applied to sprayed condensed milk. $\phi = 30^\circ$.

* Dr.-Ing. U. Manasse, Universität Bremen, Verfahrenstechnik/Fachbereich 4, Postfach 330440, 28334 Bremen (Federal Republic of Germany); present address: INVENT GmbH, Am Weichselgarten 21, 91058 Erlangen (Federal Republic of Germany).

** Dr.-Ing. T. Wriedt, Prof. Dr.-Ing. K. Bauckhage, Universität Bremen, Verfahrenstechnik/Fachbereich 4, Postfach 330440, 28334 Bremen (Federal Republic of Germany).

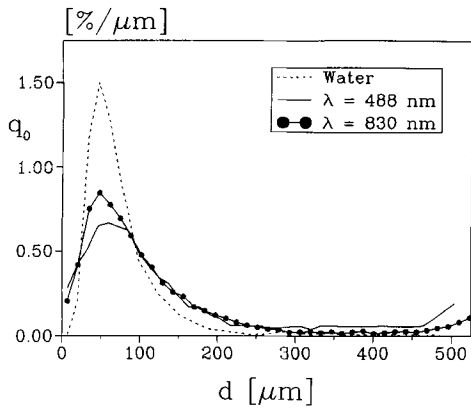


Fig. 2: Size distributions achieved by PDA applied to sprayed instant coffee. $\varphi = 30^\circ$.

the inhomogeneities inside the droplets is less pronounced when using the higher wavelength, the size distributions remain broad and unphysically large droplets are registered. Although these large droplets appear only in a small amount in the number density distribution, they influence strongly the volume density distribution, as compared in Figures 3 a and b for the sprayed water and instant coffee solution, respectively. The calculated volume fluxes would differ greatly from each other.

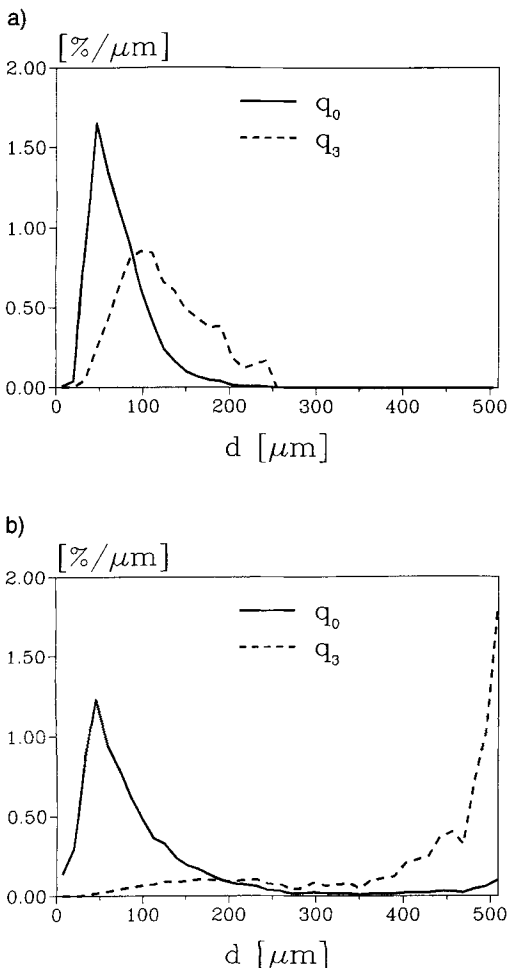


Fig. 3: Number density (q_0) and volume density distribution (q_3) as a PDA result for (a) sprayed water and (b) sprayed instant coffee.

3 Droplet Generator Results

To investigate the broadening of the particle size distributions, some PDA experiments were conducted using a piezo electric droplet generator to produce a stream of monodisperse droplets. The PDA parameters were the same as before and given in Table 1. Photography served as a reference method.

Table 1: Parameters of the PDA set-up.

Transmitter	
Laser wavelength, λ	830 nm
Beam diameter	1.3×4.0 mm
Beam diameter after expansion	1.3×4.0 mm
Focal length, f , of the front lens	750 mm
Beam intersection angle, θ	2.36°
Measuring volume:	
d_x	9621 μm
d_y	740 μm
d_z	190 μm
Receiver	
Off-axis angle, φ	30°
Diameter of aperture	36.0 mm
Distance of detector	750 mm
Elevation angle, ψ	1.45°
Size range: refraction	526 μm
reflection	420 μm

Although the droplets of the condensed milk solution and the instant coffee solution are, according to the photographs, just as monodisperse as the water droplets, the measured size distributions are broad (see Figures 4 and 5). However, the peak values of the measured size distributions correspond well with

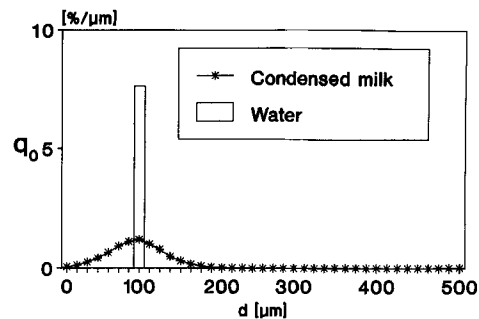


Fig. 4: Size distribution achieved by PDA applied to monodisperse condensed milk droplets. $\lambda = 830$ nm; $\varphi = 30^\circ$.

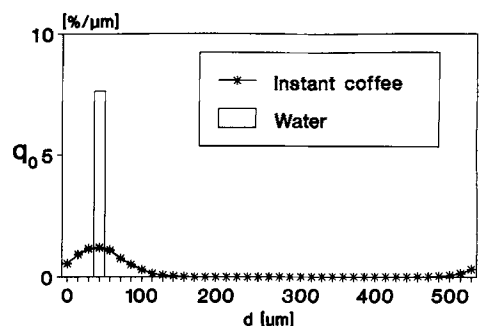


Fig. 5: Size distribution achieved by PDA applied to monodisperse instant coffee droplets. $\lambda = 830$ nm; $\varphi = 30^\circ$.

the diameters achieved by photography. Since the measurement range is restricted to 0–360°, negative phase differences result in an extra number of large particles at the end of the size range. Varying the diameter of the generated droplets by changing the orifice plates delivered size distributions with virtually the same shape. Therefore, it is concluded that the optically caused broadening of the distribution is independent of the size.

4 “Monodisperse” Spray Results

Monodisperse single droplets passing through the centre of the PDA measuring volume correspond to ideal measurement conditions. In practice, the droplets also pass outside the centre of the measuring volume, hence the influence of the Gaussian beam profile can become noticeable [3]. In addition, besides a droplet travelling through the measuring volume, further droplets sometimes move through the laser beams or the scattered light cone, thereby possibly disturbing the scattering process. Therefore, in a second step, PDA was applied to “monodisperse” sprays of the condensed milk and instant coffee solutions using charging techniques [4, 5]. The measured size distributions are plotted in Figures 6 and 7. It can be seen that the shapes of the measured size distributions belonging to the “monodisperse” spray and to the stream of monodisperse droplets are nearly the same. On the basis of these results, it is assumed that the PDA represents every size class in the form of a size-independent broadened distribution that can be determined by droplet generator experiments.

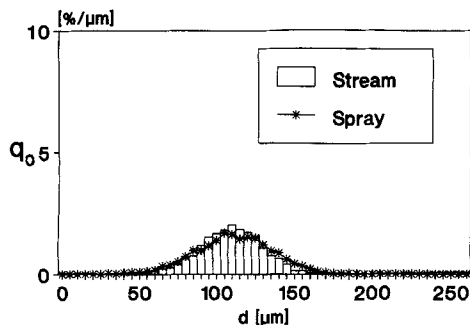


Fig. 6: Size distributions achieved by PDA applied to a stream and a spray of monodisperse condensed milk droplets. $\lambda = 830 \text{ nm}$; $\varphi = 30^\circ$.

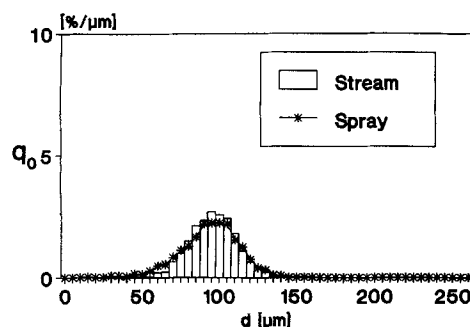


Fig. 7: Size distributions achieved by PDA applied to a stream and a spray of monodisperse instant coffee droplets. $\lambda = 830 \text{ nm}$; $\varphi = 30^\circ$.

5 Simulation of the PDA-Sizing Results

The previous experiments have shown that the measured broad size distributions are superimposed by the broad size distribution representing a size class. On the basis of a size-independent

broadening it was assumed that the measured size distributions of the sprayed process fluids are the result of the drop size distribution of water (atomized and measured under identical conditions) convoluted with the droplet generator distributions of the respective process fluid according to the equation

$$m(d) = r(d) \cdot p(d) = \int_0^{d_{\max}} r(x') p(d - x') dx', \quad (1)$$

where:

- m size distribution measured for the sprayed process fluid,
- r real size distribution, here assumed to be equal to the water spray size distribution,
- p (point spread function): size distribution achieved by PDA sizing of monodisperse process fluid droplets.

The measured and convoluted size distributions achieved with a laser wavelength of 488 nm for the solutions of instant coffee (Figure 8) and condensed milk (Figure 9) are compared. Moreover, to prove that this convolution method is also valid for other laser wavelengths, corresponding results are shown for a wavelength of 830 nm (see Figures 10 and 11). Since the measurement range is restricted to 0–360°, again negative phase differences as a result of convolution give an extra number of large particles at the end of the size range. In summary, the agreement between the measured and the calculated size distributions is fairly good.

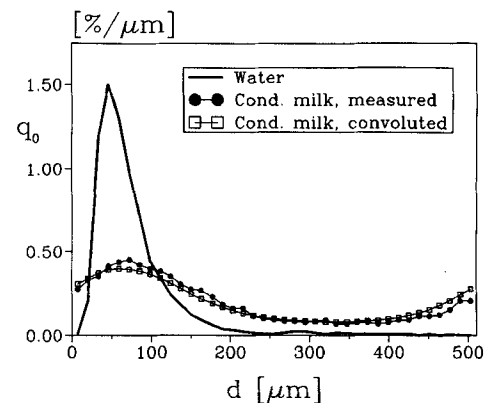


Fig. 8: Water spray droplet distribution convoluted with condensed milk droplet generator experiment result compared with measured condensed milk spray droplet distribution. $\lambda = 488 \text{ nm}$; $\varphi = 30^\circ$.

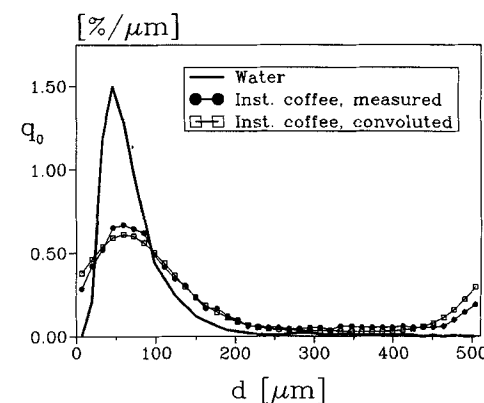


Fig. 9: Water spray droplet distribution convoluted with instant coffee droplet generator experiment result compared with measured instant coffee spray droplet distribution. $\lambda = 488 \text{ nm}$; $\varphi = 30^\circ$.

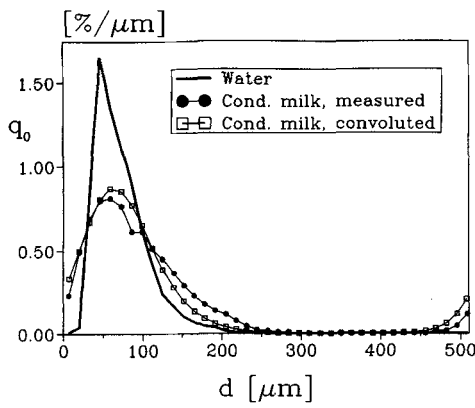


Fig. 10: Water spray droplet distribution convoluted with condensed milk droplet generator experiment result compared with measured condensed milk spray droplet distribution. $\lambda = 830 \text{ nm}$; $\varphi = 30^\circ$.

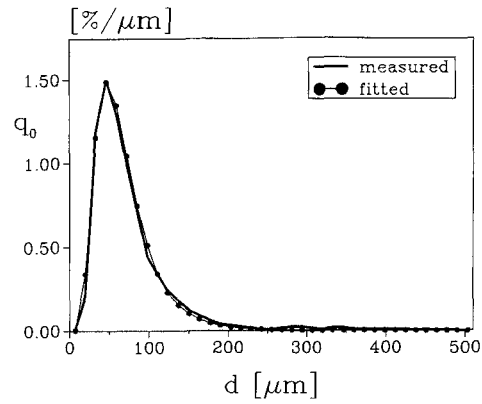


Fig. 12: Measured water spray droplet distribution fitted by a log-normal distribution function.

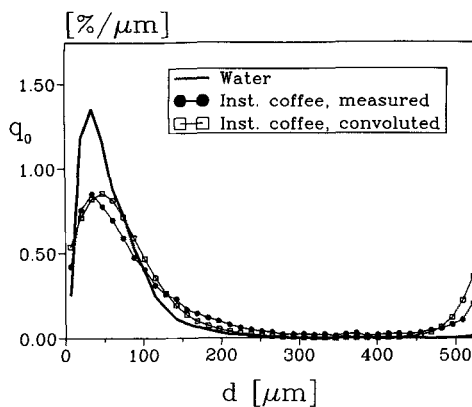


Fig. 11: Water spray droplet distribution convoluted with instant coffee droplet generator experiment result compared with measured instant coffee spray droplet distribution. $\lambda = 830 \text{ nm}$; $\varphi = 30^\circ$.

6 Deconvolution Method

Since the relationship

$$FT[m(d)] = FT[r(d) \cdot p(d)] = FT[r(d)] \cdot FT[p(d)] \quad (2)$$

exists for the Fourier transform of the convolution [6], it should be possible to obtain the real size distribution $r(d)$ by deconvolution according to the equation

$$FT[r(d)] = \frac{FT[m(d)]}{FT[p(d)]} \quad (3)$$

and following inverse Fourier transformation. Although noise was accounted for by using Wiener filtering [7], the deconvoluted distributions showed unwanted fictional peaks. Therefore, this method was discarded.

Since the measured water size distributions $w(d)$ can be well approximated by a logarithmic normal distribution function:

$$w(d) = \frac{1}{d(2\pi)^{0.5} \ln \sigma_{LN}} \exp \left[-\frac{(\ln d - \ln \bar{d})^2}{2(\ln \sigma_{LN})^2} \right] \quad (4)$$

(Figure 12), it is assumed that the real size distributions for the process fluids can also be approximated by this function. Using an evolutionary strategy [8], the two parameters of this distribu-

tion, i.e. the geometric mean diameter \bar{d} and σ_{LN} , the standard deviation of $\ln d$, are optimized in such a way that the mean square error between this log-normal distribution, convoluted with the size distribution $p(d)$ achieved by PDA sizing of the monodisperse condensed milk or of the instant coffee droplets, and the measured size distribution for their sprays is minimized. The resulting “real” size distributions of the sprayed solutions of condensed milk and instant coffee using laser wavelengths of 488 and 830 nm are shown in Figures 13–16. The reconstructed “real” size distributions are, as expected, very similar to the size

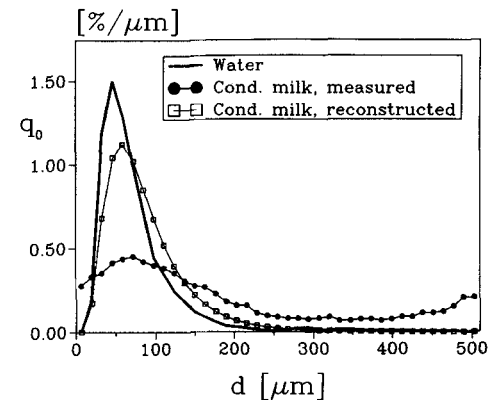


Fig. 13: “Real” sprayed condensed milk droplet size distribution as a result of reconstruction by evolutionary optimization. $\lambda = 488 \text{ nm}$; $\varphi = 30^\circ$.

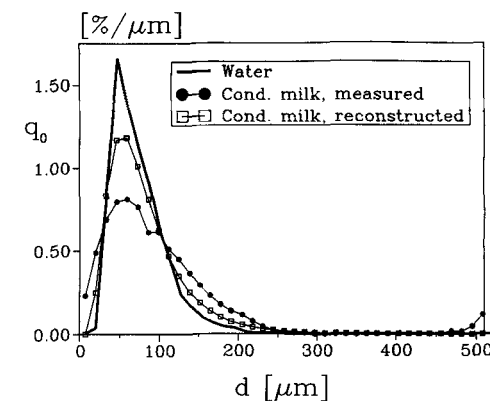


Fig. 14: “Real” sprayed condensed milk droplet size distribution as a result of reconstruction by evolutionary optimization. $\lambda = 830 \text{ nm}$; $\varphi = 30^\circ$.

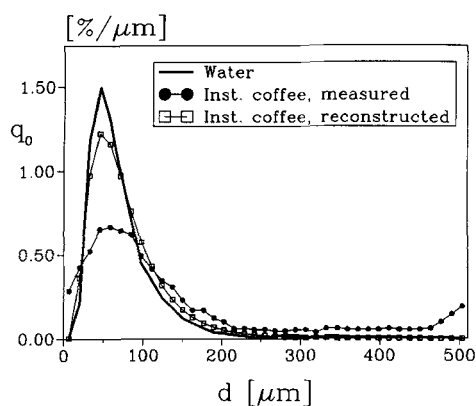


Fig. 15: "Real" sprayed instant coffee droplet size distribution as a result of reconstruction by evolutionary optimization. $\lambda = 488 \text{ nm}$; $\varphi = 30^\circ$.

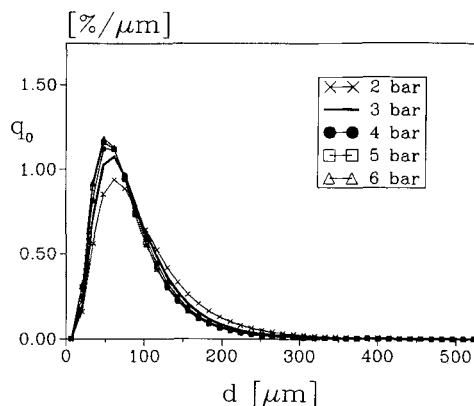


Fig. 17: Water spray size distributions for various pressures. $\lambda = 830 \text{ nm}$; $\varphi = 30^\circ$.

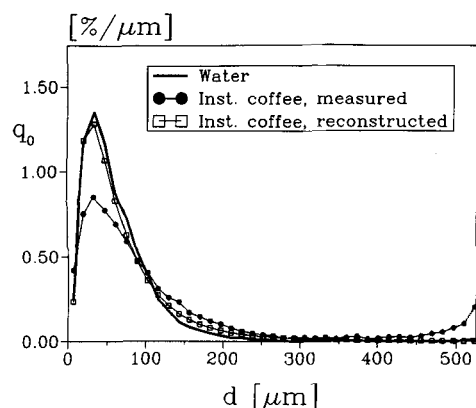


Fig. 16: "Real" sprayed instant coffee droplet size distribution as a result of reconstruction by evolutionary optimization. $\lambda = 830 \text{ nm}$; $\varphi = 30^\circ$.

distribution belonging to sprayed water. In Table 2 the characteristic parameters belonging to the log-normal distributions are summarized. At a laser wavelength of 830 nm the PDA measurements in the spray cone of the instant coffee solution were carried out with a higher sensitivity. Therefore, additional PDA measurements in the water spray cone were conducted with the same sensitivity. On the whole, the reconstruction procedure seems to be a general tool, since it delivers similar size distributions for both laser wavelengths.

Table 2: Parameters of the calculated log-normal distributions.

Fluid	$\lambda = 488 \text{ nm}$		$\lambda = 830 \text{ nm}$	
	\bar{d} (μm)	σ	\bar{d} (μm)	σ
Water	60.6	1.6	51.9	2.1
Condensed milk	76.1	1.7	71.3	1.7
Instant coffee	67.2	1.8	53.4	2.2

A criterion for the correctness of the reconstruction procedure is that the achieved size distributions should reflect changes in the spraying parameters in the right way. For atomization by means of a fan spray nozzle it is known that the mean diameter decreases with increasing pressure. Figure 17 confirms this for sprayed water. Figure 18 shows (a) the measured and (b) the

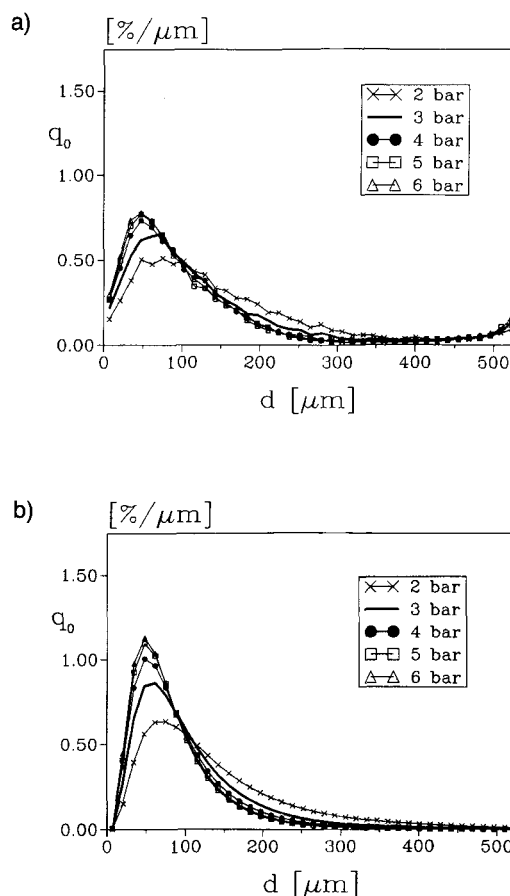


Fig. 18(a): Measured instant coffee spray size distributions for various pressures. $\lambda = 830 \text{ nm}$, $\varphi = 30^\circ$. (b) Reconstructed "real" instant coffee spray size distributions for various pressures. $\lambda = 830 \text{ nm}$, $\varphi = 30^\circ$.

reconstructed "real" size distributions for the sprayed instant coffee solution. The measured size distributions are very broad and contain very large droplets. Although the trend that with increasing pressure the peak moves to smaller diameters can be seen, these size distributions allow no declaration of mean droplet diameters or from this mean volume diameters. The reconstructed size distributions are narrower and do not contain any very large droplets. Since the mean diameter decreases with increasing pressure, it reflects and quantifies changes in the spraying parameters in the right way. The same holds for the sprayed condensed milk solution (see Figure 19a and b).

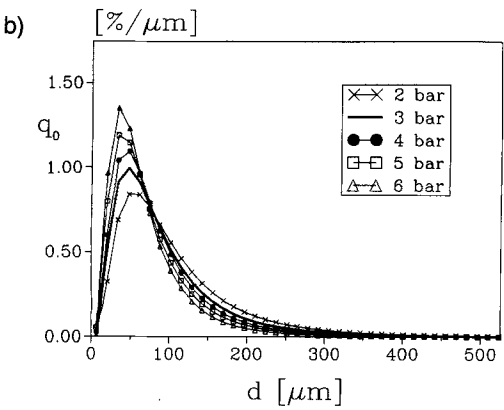
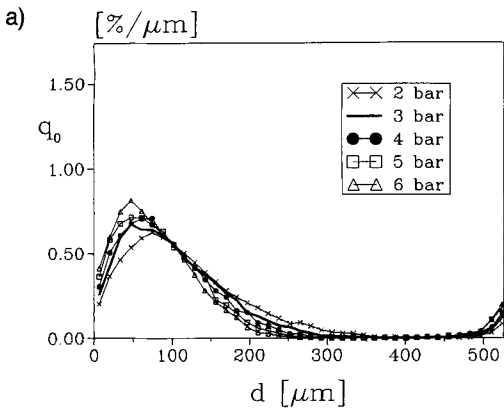


Fig. 19(a): Measured condensed milk spray size distributions for various pressures. $\lambda = 830 \text{ nm}$; $\varphi = 30^\circ$. (b) Reconstructed "real" condensed milk spray distributions for various pressures. $\lambda = 830 \text{ nm}$; $\varphi = 30^\circ$.

The result of the reconstruction method depends on the size distributions measured for the monodisperse droplets and the spray. The sensitivity and therefore the accuracy of this reconstruction method will be shown qualitatively by modifying these size distributions, respectively. In Figure 20 the PDA size distributions measured for *monodisperse condensed milk droplets* and its modification, simulating a better operation of the droplet generator or a higher sensitivity of the PDA receivers, are shown. Figure 21 shows the reconstructed size distributions for the sprayed condensed milk solution based on the measured

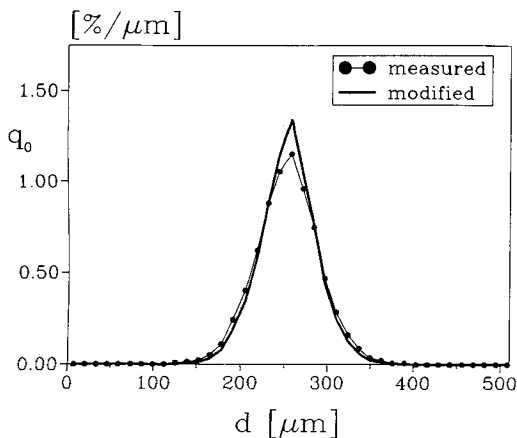


Fig. 20: Size distribution achieved by PDA applied to monodisperse condensed milk droplets and its modification. $\lambda = 830 \text{ nm}$; $\varphi = 30^\circ$.

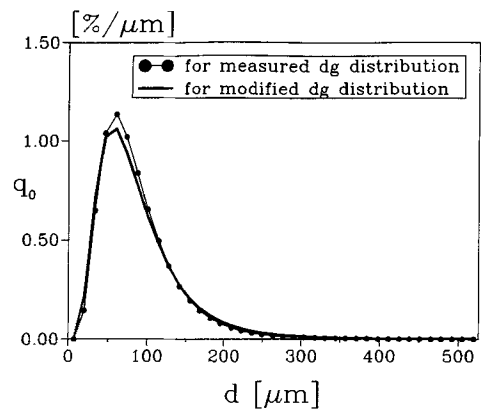


Fig. 21: Spray size distribution as a result of reconstruction by evolutionary optimization based on the modified droplet generator (dg) distribution. $\lambda = 830 \text{ nm}$; $\varphi = 30^\circ$.

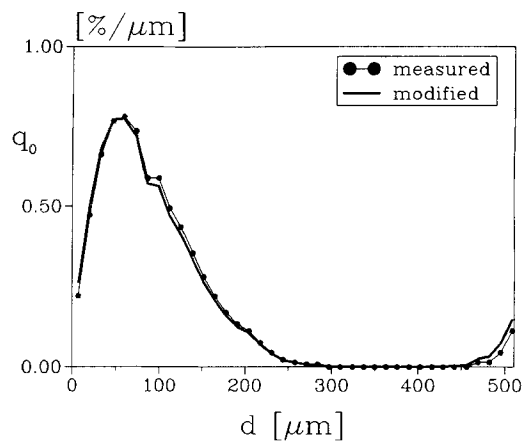


Fig. 22: Size distribution achieved by PDA applied to a spray of condensed milk and its modification. $\lambda = 830 \text{ nm}$; $\varphi = 30^\circ$.

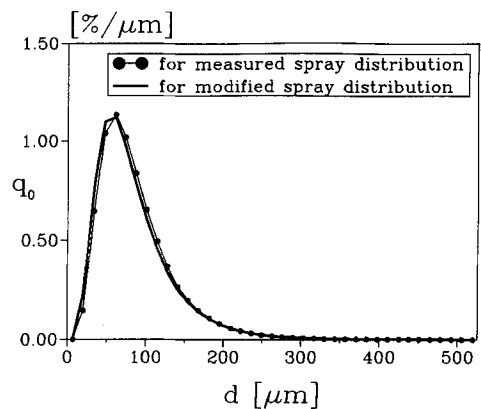


Fig. 23: Spray size distribution as a result of reconstruction by evolutionary optimization based on the modified spray size distribution. $\lambda = 830 \text{ nm}$; $\varphi = 30^\circ$.

and the modified droplet generator distributions. The two distributions differ only very slightly. In Figure 22, the modification was that the PDA measurement for the *sprayed condensed milk* was conducted with a higher sensitivity of the PDA receivers, which makes more small particles detectable. Again the reconstructed size distributions differ only very slightly (see Figure 23).

7 Conclusions

The results show that by using reconstruction methods such as those described in this paper, information about the “real” size distributions of sprayed process fluids is accessible. This allows model experiments to be conducted using laboratory (for research and development) instead of in situ measurements and permits the transfer of these results from the laboratory to, for example, a spray dryer plant. Consequently, PDA can be applied to real process fluids and can be used for process control.

8 Acknowledgement

The authors gratefully acknowledge the financial support of this work by the Deutsche Forschungsgemeinschaft, Bonn/Bad Godesberg.

9 Symbols and Abbreviations

d	particle diameter
m	size distribution measured for the sprayed process fluid
p	size distribution achieved by PDA-sizing of monodisperse process fluid droplets
q_0	number density distribution
q_3	volume density distribution
r	real size distribution
θ	beam intersection angle
γ	light wavelength

σ	standard deviation
Φ	phase difference
ψ	elevation angle
ϕ	off-axis angle

10 References

- [1] *U. Manasse, T. Wriedt, K. Bauckhage*: Phase-Doppler sizing of optically absorbing liquid droplets: comparison between Mie theory and experiment. *Part. Part. Syst. Charact.* 9 (1992) 176–185.
- [2] *U. Manasse, T. Wriedt, K. Bauckhage*: Phase Doppler sizing of optically absorbent single- and multicomponent liquid droplets using semiconductor devices. *Meas. Sci. Technol.* 4 (1993) 369–377.
- [3] *G. Gréhan, G. Gouesbet, A. Naqwi, F. Durst*: Trajectory ambiguities in phase Doppler systems: use of polarizers and additional detectors to suppress the effect. *Proc. Sixth Int. Symp. on Applications of Laser Anemometry to Fluid Mechanics*, Lisbon, Portugal, July 20–23, 1992, pp. 12.1.1–12.1.7.
- [4] *K.-J. Choi, B. Delcorio*: Generation of controllable monodispersed sprays using impulse jet and charging techniques. *Rev. Sci. Instrum.* 61 (1990) 1689–1693.
- [5] *M. Berg*: Untersuchungen zur Erzeugung von monodispersen Sprays durch Anlegen eines elektrostatischen Feldes entlang einer nach dem Rayleigh’schen Strahlzerfallsprinzip erzeugten monodispersen Tropfenkette. Studienarbeit, Universität Bremen/FB4, 1993.
- [6] *J. W. Goodman*: Introduction to Fourier Optics. McGraw-Hill, San Francisco 1968.
- [7] *W. H. Press, B. P. Flannery, S. A. Teukolsky, W. T. Vetterling*: Numerical Recipes, Cambridge, MA, 1986.
- [8] *H. Schmiedel*: Anwendung der Evolutionsoptimierung bei Mikrowellenschaltungen. *Frequenz* 35 (1981) 306–310.